Improved Kármán-Pohlhausen Momentum-Integral Approximations for Non-Newtonian Boundary Layers over a Flat Plate

Suzanne R. Feist* and Joseph Majdalani†
Auburn University, Auburn, AL 36849

In this work, an integral formulation is developed for the laminar boundary layer associated with the steady incompressible motion of non-Newtonian power-law fluids over flat plates. To this end, the Kármán–Pohlhausen momentum-integral approach is used to approximate boundary-layer growth and skin-friction characteristics under zero pressure-gradient conditions. This is accomplished using Pohlhausen's classic fourth-order velocity profile in addition to an optimal (MX4) quartic polynomial approximation for the nearfield velocity (Majdalani, J., and Xuan, L.-J., "On the Kármán Momentum-Integral Approach and the Pohlhausen Paradox," Physics of Fluids, Vol. 32, No. 12, 2020, p. 123605). Using a power-law relation between the normal velocity gradient and shear stress, model-based predictions of fundamental boundary-layer properties are evaluated and compared to an 'exact' similarity solution that can be computed numerically. Since the power-law constitutive relation retains the flow-behavior index, n, as a general parameter, closed-form analytical expressions are provided for most boundary-layer properties as functions of the streamwise position and n. These include the disturbance, displacement, and momentum thicknesses, as well as the local skin-friction coefficient, and wall-normal velocity. By way of verification, the resulting formulations are shown to compare well to the exact similarity solution and to readily recover the traditional Newtonian expressions in the appropriate limit of $n = 1$. They also enable us to quantify the sensitivity of the boundary-layer thickness and skin friction coefficient in shear-thinning and shear-thickening fluids depending on the value of n. Overall, the MX4 profile is found to be highly accurate for flow-behavior indexes of 0.88 and higher, namely, for nearly Newtonian and all dilatant fluids. Conversely, the accuracy of Pohlhausen's fourth-order polynomial profile is seen to improve as n is decreased below 0.88, hence making it more suitable for shear-thinning or pseudoplastic fluids.

Nomenclature

C_f	local skin-friction coefficient
$F(\eta)$	dimensionless velocity profile
$F'(0)$	wall velocity-gradient parameter, F'_0
H	shape factor, δ^*/θ
K	consistency coefficient for a power-law fluid
n	flow-behavior index for a power-law fluid
Re_x	local Reynolds number based on streamwise distance
U_∞	freestream velocity
(u, v)	velocity components in streamwise and wall-normal directions
(x, y)	streamwise and wall-normal coordinates

Greek

α	displacement-thickness ratio, δ^*/δ
β	momentum-thickness ratio, θ/δ
δ	boundary-layer (disturbance) thickness
δ^*	displacement thickness
η	similarity coordinate, y/δ
θ	momentum thickness
μ	dynamic viscosity
ν	kinematic viscosity
ρ	fluid density
τ_w	wall shear stress

*Undergraduate Research Assistant, Department of Aerospace Engineering, AIAA University Student Member 1923968.
†Professor and Francis Chair, Department of Aerospace Engineering, AIAA Lifetime Fellow 199546.

I. Introduction

LAMINAR boundary layers developing over flat plates constitute one of the most fundamental canonical problems in viscous fluid mechanics [1]. Beyond their theoretical elegance, they form the basis of countless engineering analyses in aerodynamics, propulsion, and convective heat transfer [1]. Following Prandtl's pioneering formulation of boundary-layer theory [2], the classical Newtonian solution, obtained through the similarity transformation introduced by Blasius [3], remains one of the most celebrated exact reductions of the Navier–Stokes equations. Its analytical structure has provided generations of researchers with reliable approximations for boundary-layer, displacement, and momentum thicknesses, as well as local skin-friction predictions.

Despite its central role, the Newtonian designation represents only a subset of practical fluids encountered in engineering systems. Many technologically relevant fluids, including polymer solutions, slurries, propellants, lubricants, and biological suspensions, exhibit rheological behavior that deviates from linear viscosity models. In such cases, the effective viscosity becomes dependent on the local shear rate, and classical boundary-layer theory must be generalized accordingly. The historical development of boundary-layer theory and transport modeling provides the foundation for such extensions [4–7].

Among the various constitutive models proposed for generalized Newtonian fluids, the Ostwald–de Waele power-law representation offers a tractable yet sufficiently flexible description of shear-thinning and shear-thickening behavior. In this model, the shear stress may be related to the local velocity gradient through

$$\tau = K\left(\frac{\partial u}{\partial y}\right)^n, \tag{1}$$

where K and n denote the consistency coefficient and flow-behavior index, which control the power-law formulation. Naturally, the Newtonian limit is recovered when $n = 1$, whereas $n < 1$ and $n > 1$ correspond to pseudoplastic and dilatant fluids, respectively. Owing to its analytical simplicity and ability to capture first-order rheological effects, the power-law model has been widely adopted in external flow and heat-transfer analyses [8–14]. Comprehensive treatments of non-Newtonian transport phenomena further showcase its practical utility [15, 16].

The introduction of nonlinear viscosity, however, fundamentally alters the character of boundary-layer development. In contrast to the Newtonian case, the coupling between the shear stress and the normal velocity gradient modifies the streamwise scaling of the disturbance thickness, the wall-shear behavior, and the structure of the velocity profile. Nevertheless, similarity reductions remain possible. Early investigations by Schowalter [8] and Acrivos et al. [9] confirm that boundary-layer equations for power-law fluids admit similarity forms. More recently, as shown by Myers [17], the boundary-layer equations for a power-law fluid over a flat plate may be reduced to a nonlinear ordinary differential equation (ODE) of the form

$$\left(|f''|^{n-1}f''\right)' + \frac{1}{n+1}ff'' = 0,$$

where the classical boundary conditions, $f(0) = f'(0) = 0$ and $f'(\infty) = 1$, which date back to Blasius [3], remain valid. The resulting similarity solution provides accurate predictions of the wall-gradient parameter $f''(0)$, from which the local skin-friction coefficient and boundary-layer thickness may be deduced. Although this approach yields benchmark-quality solutions, it generally requires numerical integration and does not produce closed-form expressions that facilitate rapid engineering design [18, 19].

For this reason, integral boundary-layer methods continue to retain practical relevance. Introduced through the seminal works of von Kármán [20] and Pohlhausen [21], the so-called Kármán–Pohlhausen (KP) momentum-integral approach reduces the boundary-layer equations to an ODE for the disturbance thickness by incorporating an assumed velocity profile in the nearfield. Despite its simplicity, the KP method has remained a staple of boundary-layer analysis and continues to be featured prominently in modern monographs [22–24]. Its analytical tractability and ability to furnish closed-form approximations under both laminar and turbulent compressible and incompressible flows make it particularly attractive for non-Newtonian extensions, where exact solutions are often unattainable.

The accuracy of integral formulations, however, depends in large part on the assumed nearfield velocity profile. In this context, Pohlhausen's quartic polynomial has been widely employed in both Newtonian and non-Newtonian contexts [11, 25]. Yet, as shown by Majdalani and Xuan [26], higher-order polynomial constructions do not necessarily improve the agreement with similarity solutions. Their analysis reveals that certain boundary conditions, most particularly the imposition of zero curvature at the boundary-layer edge, will invariably degrade predictive accuracy in Newtonian fluids. By relaxing this overly restrictive edge constraint and, instead, optimizing the wall-gradient parameter, an improved quartic representation (MX4) is attained; the latter not only overcomes the so-called Pohlhausen paradox, it also agrees more substantially with the Blasius solution while retaining analytical simplicity [26].

So far, extensions of the Kármán–Pohlhausen framework to non-Newtonian fluids have been pursued in numerous configurations, including forced convection over planar, axisymmetric, and irregular geometries [27–29], natural convection in porous media [30, 31], slider-bearing flows [32], radial films [33], and mixed convection around cylinders [34]. Although integral methods have been extended to power-law fluids in some configurations [11], a systematic evaluation of the relative performance of classical and optimized polynomial profiles across the full range of flow-behavior indices remains, however, unexplored. In particular, it is not yet fully established how shear-thinning and shear-thickening behavior affects the predictive fidelity of integral boundary-layer approximations relative to the similarity solution of Myers [17]. Because wall shearing in a power-law fluid scales with the velocity gradient raised to the power n, even modest discrepancies in the wall gradient estimation can be amplified in dilatant regimes. Conversely, shear-thinning behavior may reduce the sensitivity to the choice of the nearfield velocity.

The objective of the present work is therefore to primarily assess the predictive capability of Kármán–Pohlhausen integral formulations for laminar power-law boundary layers over a flat plate under zero pressure-gradient conditions. To this end, two assumed velocity distributions will be considered: the classical Pohlhausen quartic profile and the optimized MX4 polynomial introduced by Majdalani and Xuan [26]. Their predictions for the fundamental boundary-layer properties, such as the disturbance, displacement, and momentum thicknesses, as well as the wall-normal velocity and skin-friction coefficient, will be evaluated explicitly and compared against the exact similarity solution, which can be safely treated as the reference model [17, 35].

More specifically, by examining a range of flow-behavior indices spanning shear-thinning, Newtonian, and shear-thickening regimes [15, 36], the present study will seek to quantify the effect of varying the rheological parameters on the predictive accuracy of integral boundary-layer approximations. Through this comparison, the analysis will seek to identify the regimes in which Pohlhausen's polynomial representation remains adequate and those in which the improved MX4 profile becomes an essential alternative.

II. Problem Formulation and Solution Procedure

A. Geometric Description and Flow Configuration

We consider the steady, two-dimensional motion of an incompressible power-law fluid over a semi-infinite flat plate aligned with a uniform freestream. The plate is assumed to be smooth, impermeable, and of negligible thickness, with its leading edge situated at $x = 0$. The streamwise coordinate, x, is measured along the plate surface, whereas the wall-normal coordinate, y, is taken perpendicular to it.

A uniform external velocity U_∞ impinges upon the plate, thereby initiating the development of a laminar boundary layer along its surface as a direct consequence of viscous momentum diffusion. Outside the viscous region, the flow remains uniformly inviscid, and no pressure gradient arises in the streamwise direction. Accordingly, the boundary-layer growth is driven exclusively by viscous transport, with no contribution from favorable or adverse pressure-gradient effects.

The fluid is modeled as a generalized Newtonian medium that is governed by the Ostwald–de Waele power-law constitutive relation that exhibits a consistency coefficient K and a flow-behavior index n. The classical Newtonian limit is recovered when $n = 1$. For $n < 1$, the model describes shear-thinning (pseudoplastic) behavior, whereas $n > 1$ corresponds to a shear-thickening (dilatant) response. In this manner, the rheological parameter n provides a continuous measure of deviation from linear viscous behavior.

The present analysis focuses on the streamwise evolution of the velocity field, the disturbance (boundary-layer) thickness, and the associated wall shear stress along the plate. The flow domain is assumed to be sufficiently large in the wall-normal direction such that the velocity asymptotically approaches the freestream value at the edge of the boundary layer. For clarity and reference, the physical configuration and the streamline-bounded control volume used in the momentum-integral formulation are depicted in Fig. 1.

B. Governing Equations

The motion of a steady, incompressible power-law fluid is prescribed by the continuity equation in conjunction with the Navier–Stokes momentum equations, supplemented by a non-Newtonian constitutive relation. For high-Reynolds-number external flow over a flat plate, the classical boundary-layer approximations can be implemented [2]. The flow

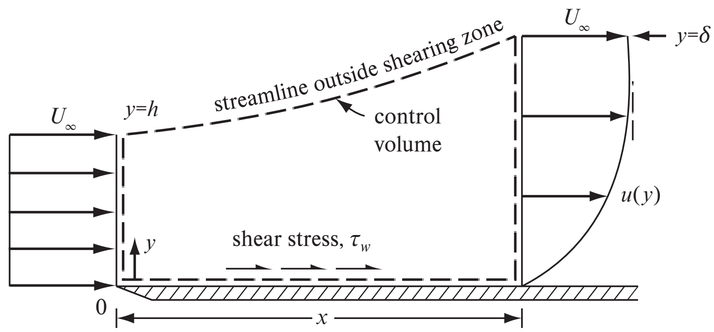

Fig. 1. Schematic of laminar boundary-layer development over a flat plate and associated control volume used in the momentum-integral analysis.

can be taken to be two-dimensional, with the streamwise velocity component dominating the motion and wall-normal gradients substantially exceeding their streamwise counterparts.

Within the viscous layer, pressure variation in the wall-normal direction remains negligible. Moreover, for a flat plate aligned with a uniform freestream, the external velocity remains spatially invariant, so that $\mathrm{d}U_\infty/\mathrm{d}x = 0$. Under these conditions, the full Navier–Stokes equations reduce to the familiar boundary-layer form, while the continuity equation retains its standard expression. The resulting system captures the essential balance between convective inertia and viscous diffusion whose interplay induces the shear-layer development along the plate.

To proceed analytically, the reduced boundary-layer equations are cast into their integral representation following the classical momentum-integral framework introduced by von Kármán [37] before becoming formalized in standard treatments of laminar boundary layers [38]. This formulation enables the streamwise evolution of the disturbance thickness to be related directly to the wall shear stress through an assumed representation of the nearfield velocity distribution. Within the boundary layer, using standard nomenclature, e.g. ρ for density, we have

$$\frac{\partial u}{\partial x} + \frac{\partial v}{\partial y} = 0 \qquad \text{and} \qquad u\frac{\partial u}{\partial x} + v\frac{\partial u}{\partial y} = U_\infty \frac{\mathrm{d}U_\infty}{\mathrm{d}x} + \frac{1}{\rho}\frac{\partial \tau_{xy}}{\partial y}. \tag{2}$$

Outside the boundary layer, the inviscid flow satisfies Euler's equation,

$$-\frac{1}{\rho}\frac{\mathrm{d}p}{\mathrm{d}x} = U_e \frac{\mathrm{d}U_e}{\mathrm{d}x}, \tag{3}$$

where $U_e(x)$ represents the external or edge velocity. For a flat plate aligned with the freestream, the external velocity remains constant, $U_e = U_\infty$, the pressure gradient vanishes, and the momentum-integral equation reduces to

$$U_\infty^2 \frac{\mathrm{d}\theta}{\mathrm{d}x} + (2\theta + \delta^*) U_\infty \frac{\mathrm{d}U_\infty}{\mathrm{d}x} = \frac{1}{\rho}\tau_w \qquad \text{or} \qquad \rho U_\infty^2 \frac{\mathrm{d}\theta}{\mathrm{d}x} = \tau_w, \tag{4}$$

where τ_w stands for the wall shear stress, and both δ^* and θ denote the displacement and momentum thicknesses, respectively. These are generally specified by

$$\delta^* = \int_0^\delta \frac{U_\infty - u}{U_\infty}\,\mathrm{d}y = \delta \int_0^1 [1 - F(\eta)]\,\mathrm{d}\eta, \quad F(\eta) \equiv \frac{u}{U_\infty} \quad \text{and} \quad \eta \equiv \frac{y}{\delta}, \tag{5}$$

$$\theta = \int_0^\delta \frac{u}{U_\infty}\frac{U_\infty - u}{U_\infty}\,\mathrm{d}y = \delta \int_0^1 F(\eta)[1 - F(\eta)]\,\mathrm{d}\eta, \qquad \text{and} \qquad H \equiv \frac{\delta^*}{\theta}, \tag{6}$$

with H referring to the shape factor. Additionally, normalized forms of δ^* and θ with the disturbance thickness δ can be readily deduced. One gets

$$\alpha \equiv \frac{\delta^*}{\delta} = \int_0^1 [1 - F(\eta)]\,\mathrm{d}\eta \quad \text{and} \quad \beta \equiv \frac{\theta}{\delta} = \int_0^1 F(\eta)[1 - F(\eta)]\,\mathrm{d}\eta, \tag{7}$$

where α and β define the non-dimensional displacement and momentum thicknesses, respectively.

C. Schowalter–Acrivos Similarity Transformation

The laminar boundary layer associated with a power-law fluid over a flat plate may be treated through a similarity transformation that reduces the boundary-layer equations to a single nonlinear ODE. This formulation furnishes a benchmark solution for the velocity distribution, wall shear stress, and boundary-layer thickness without invoking an assumed nearfield velocity profile. As such, it serves as a rational standard against which integral approximations can be assessed. By introducing an appropriate similarity variable, $\xi = y\sqrt{\nu x/U_\infty}$, together with a streamfunction representation, $f(\xi) = \psi/\sqrt{\nu x U_\infty}$, the boundary-layer equations collapse into a self-similar structure. The resulting transformation reduces the streamwise momentum equation to a generalized Blasius equation for an Ostwald–de Waele power-law fluid [17]. The resulting Schowalter–Acrivos similarity equation can be written as [8, 9]:

$$\left(|f''|^{n-1}f''\right)' + \frac{1}{n+1}ff'' = 0; \quad f(0) = f'(0) = 0, \quad f'(\infty) = 1. \tag{8}$$

This solution yields the wall-gradient parameter, $f''(0)$, from which the skin friction may be estimated, specifically,

$$C_f(x)Re_x^{\frac{n}{n+1}} = 2\left[f''(0)\right]^n; \qquad Re_x \equiv \rho U_\infty^{2-n}x/K, \tag{9}$$

where Re_x denotes the generalized Reynolds number and the differentiation in this case is carried out with respect to ξ.

D. The Quartic Kármán–Pohlhausen (KP4) Polynomial Profile

The classical Kármán–Pohlhausen approach assumes a polynomial representation of the velocity distribution within the boundary layer [1, 39]. In fact, the use of polynomial profiles to model boundary layers is frequently attempted in both laminar and turbulent formulations [40, 41]. One of the most widely relied upon quartic profiles —dating back to Pohlhausen [21]— may be given by

$$F(\eta) = \frac{u}{U_\infty} = 2\eta - 2\eta^3 + \eta^4; \qquad \eta \equiv \frac{y}{\delta} \qquad \text{and} \qquad F_0' \equiv F'(0) = 2 \qquad \text{(KP4)}. \tag{10}$$

This KP4 distribution satisfies five conditions postulated by Pohlhausen [21]. These consist of (1) no wall slippage, (2) freestream velocity matching at $y = \delta$, (3) vanishing shear at $y = \delta$, (4) vanishing pressure gradient at $y = \eta = 0$ (in the nearfield momentum equation), and (5) vanishing shear stress gradient at $y = \delta$. Mathematically, we have:

$$u(0) = 0, \qquad u(\delta) = U_\infty, \qquad \left.\frac{\partial u}{\partial y}\right|_{y=\delta} = 0, \qquad \left.\frac{\partial^2 u}{\partial y^2}\right|_{y=0} = 0, \qquad \left.\frac{\partial^2 u}{\partial y^2}\right|_{y=\delta} = 0. \tag{11}$$

In view of KP4 in Eq. (10), the displacement and momentum thicknesses can be evaluated directly from Eqs. (5) and (6). Alternatively, in dimensionless form, one may use Eq. (7) to collect

$$\alpha = \frac{\delta^*}{\delta} = \frac{3}{10} \quad \text{and} \quad \beta = \frac{\theta}{\delta} = \frac{37}{315}. \tag{12}$$

These relations will be later substituted into the power-law expressions for boundary-layer thickness growth and skin-friction integrals before undertaking comparisons with other formulations and the exact Schowalter–Acrivos solution.

E. The Quartic Majdalani–Xuan (MX4) Polynomial Profile

In recent investigations of Newtonian boundary layers [26, 42, 43], the MX4 quartic distribution is shown to outperform the KP4 in estimating both hydrodynamic and thermal boundary-layer properties. This fourth-order MX4 polynomial profile can be written as

$$F(\eta) = \frac{5}{3}\eta - \eta^3 + \frac{1}{3}\eta^4; \qquad F_0' = \frac{5}{3} \qquad \text{(MX4)}. \tag{13}$$

In practice, the MX4 profile satisfies all but the last boundary condition in Eq. (11), namely, that postulated without proof by Pohlhausen [21]. According to Majdalani and Xuan [26], the latter stands at the root of the Pohlhausen paradox; it can be readily shown to be rather incompatible with the corresponding value derived from the exact Blasius solution. After confirming its incongruence with the Blasius solution, it is relaxed while deriving MX4. The resulting quartic form provides sufficient flexibility to capture the curvature of the velocity profile across the boundary layer region while maintaining an analytical structure that is suitable for closed-form evaluation of the displacement and momentum thickness integrals. For example, by substituting MX4 into Eq. (7), one readily retrieves

$$\alpha = \frac{\delta^*}{\delta} = \frac{7}{20} \quad \text{and} \quad \beta = \frac{\theta}{\delta} = \frac{379}{2835}, \tag{14}$$

which fall within a fraction of one percent of their exact values.

F. Wall Shear Stress for a Power-Law Fluid

For non-Newtonian fluids described by the power-law model [17], the shear stress may be related to the rate of deformation through

$$\tau = K\left(\frac{\partial u}{\partial y}\right)^n \qquad \text{and so} \quad \tau_w = K\left(\left.\frac{\partial u}{\partial y}\right|_{y=0}\right)^n. \tag{15}$$

where K and n denote the consistency coefficient and flow-behavior index, respectively. This relation represents a generalized constitutive law in which the apparent viscosity depends on the local shearing rate. For $n < 1$ (shear-thinning fluids), τ_w increases gradually with successive increases in the velocity gradient, and this may be attributed to the reduced effective viscosity at higher shearing rates. Conversely, for $n > 1$ (shear-thickening fluids), τ_w increases more rapidly with the velocity gradient, given the corresponding increase in effective viscosity. This constitutive relation between the velocity field and τ_w will enable us to close the momentum-integral formulation for non-Newtonian boundary-layer flows [11]. For an arbitrary velocity profile, including those given by Eqs. (10) and (13), one can put

$$\frac{\partial u}{\partial y} = \frac{U_\infty}{\delta}F'(\eta), \qquad \left.\frac{\partial u}{\partial y}\right|_{y=0} = \frac{U_\infty}{\delta}F'(0) = \frac{F_0' U_\infty}{\delta}, \qquad \text{and so} \qquad \tau_w = K\left(\frac{F_0' U_\infty}{\delta}\right)^n. \tag{16}$$

G. Generalized Disturbance Thickness and Skin-Friction Coefficient

At this juncture, one may substitute $\theta = \beta\delta$ from Eq. (7) and τ_w from Eq. (16) into the momentum-integral equation given by Eq. (4). One recovers

$$\rho U_\infty^2 \beta \frac{\mathrm{d}\delta}{\mathrm{d}x} = K\left(\frac{F_0' U_\infty}{\delta}\right)^n, \quad \delta^n \frac{\mathrm{d}\delta}{\mathrm{d}x} = \frac{K}{\beta\rho}\left(F_0'\right)^n U_\infty^{n-2}, \quad \text{and so} \quad \delta^{n+1} = \frac{(n+1)K}{\beta\rho}\left(F_0'\right)^n U_\infty^{n-2}x. \tag{17}$$

In this manner, the boundary-layer thickness may be determined for arbitrary consistency coefficient and flow-behavior index using

$$\delta(x) = \left[\frac{(n+1)K}{\beta\rho}F_0'^n\right]^{\frac{1}{n+1}} U_\infty^{\frac{n-2}{n+1}} x^{\frac{1}{n+1}}, \tag{18}$$

where, as before, $F_0' = F'(0)$. As for the local skin-friction coefficient, it may be immediately constructed from

$$C_f(x) = \frac{\tau_w}{\frac{1}{2}\rho U_\infty^2} = 2\left(\frac{\beta F_0'}{n+1}\right)^{\frac{n}{n+1}}\left(\frac{K}{\rho}\right)^{\frac{1}{n+1}} U_\infty^{\frac{n-2}{n+1}} x^{-\frac{n}{n+1}}. \tag{19}$$

Since it is customary to express δ and C_f in terms of Re_x, we introduce its more generalized n-dependent expression, $Re_x \equiv \rho U_\infty^{2-n} x/K$. After some rearrangements, we obtain the normalized universal forms:

$$\frac{\delta(x)}{x} Re_x^{\frac{1}{n+1}} = \left(\frac{n+1}{\beta}F_0'^n\right)^{\frac{1}{n+1}} = a \quad \text{and} \quad C_f(x) Re_x^{\frac{n}{n+1}} = 2\left(\frac{\beta F_0'}{n+1}\right)^{\frac{n}{n+1}} = b. \tag{20}$$

where a and b denote characteristic constants. For the KP4 and MX4 profiles, as an example, one simply gets

$$\delta(x) = \left[\frac{(n+1)K}{\frac{37}{315}\rho}2^n\right]^{\frac{1}{n+1}} U_\infty^{\frac{n-2}{n+1}} x^{\frac{1}{n+1}} \quad \text{(KP4)} \quad \text{and} \quad \delta(x) = \left[\frac{(n+1)K}{\frac{379}{2835}\rho}\left(\frac{5}{3}\right)^n\right]^{\frac{1}{n+1}} U_\infty^{\frac{n-2}{n+1}} x^{\frac{1}{n+1}} \quad \text{(MX4)}, \tag{21}$$

and, for the skin friction,

$$C_f = 2\left(\frac{\frac{74}{315}}{n+1}\right)^{\frac{n}{n+1}} \left(\frac{K}{\rho}\right)^{\frac{1}{n+1}} U_\infty^{\frac{n-2}{n+1}} x^{-\frac{n}{n+1}} \quad \text{(KP4)} \quad \text{and} \quad C_f = 2\left(\frac{\frac{379}{1701}}{n+1}\right)^{\frac{n}{n+1}} \left(\frac{K}{\rho}\right)^{\frac{1}{n+1}} U_\infty^{\frac{n-2}{n+1}} x^{-\frac{n}{n+1}} \quad \text{(MX4)}. \tag{22}$$

Unsurprisingly, when $n = 1$, the solution reduces to the classical flat-plate scaling with $\delta \sim x^{1/2}$ and $C_f \sim x^{-1/2}$.

H. Wall-Normal Velocity

In order to assess the degree of transverse mass transport, the wall-normal velocity may be extracted and expressed in closed form. By substituting $u = U_\infty F(\eta)$ into the continuity equation, one gets

$$\frac{v}{U_\infty} = \frac{\delta(x)}{(n+1)x} \int_0^\eta s\, F'(s)\ \mathrm{d}s, \tag{23}$$

so that the normalized transverse velocity becomes

$$\hat{v}(\eta) \equiv \left(\frac{v}{U_\infty}\right) Re_x^{\frac{1}{n+1}} = \frac{1}{n+1}\left[\frac{\delta(x)}{x} Re_x^{\frac{1}{n+1}}\right] \int_0^\eta s\, F'(s)\ \mathrm{d}s. \tag{24}$$

For the KP4 and MX4 profiles at the boundary-layer edge ($\eta = 1$), we have

$$\int_0^1 s\, F_P'(s)\ \mathrm{d}s = \eta^2 - \frac{3}{2}\eta^4 + \frac{4}{5}\eta^5 = \frac{3}{10} \text{ (KP4)} \quad \text{and} \quad \int_0^1 s\, F_M'(s)\ \mathrm{d}s = \frac{5}{6}\eta^2 - \frac{3}{4}\eta^4 + \frac{4}{15}\eta^5 = \frac{7}{20} \text{ (MX4)}. \tag{25}$$

In what follows, comparisons will be carried out between the similarity solution and both KP4 and MX4 predictions.

III. Results and Discussion

The predictive accuracy of the integral boundary-layer formulations is now assessed by comparing results obtained using the classical Pohlhausen quartic and the optimized MX4 velocity profiles against the similarity solution for a non-Newtonian flow over a flat plate. The similarity solution is treated as the reference model, as it does not rely on an assumed nearfield velocity distribution. It may be viewed as reflecting the true rheological scaling of the constitutive equations. Predictions of displacement thickness, momentum thickness, disturbance growth, and local skin-friction coefficient are subsequently evaluated over a representative range of flow-behavior indices.

We begin with Table 1, which delineates the structural differences between the similarity solution and the polynomial approximations. While the similarity solution captures the dependence of the displacement and momentum thickness ratios on the flow-behavior index n, both polynomial profiles, by construction, yield constant values of α, β, and H. This invariance reflects the fact that the assumed velocity distributions impose a fixed geometric structure on the boundary layer. In contrast, the similarity formulation accommodates the evolving balance between inertial transport and nonlinear viscous diffusion as rheological effects vary with n. The distinction is fundamental: the integral approach adapts to the non-Newtonian motion, whereas the similarity solution prescribes it.

The quantitative implications of this structural difference are summarized in Table 2. Therein, deviations in boundary-layer growth and skin-friction scaling are reported relative to the similarity solution. The smallest discrepancies occur near the Newtonian limit ($n \approx 1$), where both polynomial profiles most closely resemble the classical laminar boundary-layer structure. This behavior may have been anticipated as both KP4 and MX4 were developed for a Newtonian fluid in mind. Away from this limit, the accuracy becomes increasingly regime dependent. The Pohlhausen profile remains competitive for shear-thinning fluids, whereas the MX4 formulation yields improved predictions of both C_f and δ as the flow transitions toward Newtonian and shear-thickening behavior.

This trend is illustrated more clearly in Fig. 2a, which presents the percent relative error in the skin-friction coefficient as a function of the flow-behavior index. In strongly shear-thinning regimes, the Pohlhausen profile exhibits smaller deviations. However, near $n \approx 0.88$, the MX4 formulation begins to track the similarity solution more closely. In the Newtonian limit and throughout the shear-thickening regime, the MX4 profile consistently outperforms the KP4 model in skin-friction estimates. This improvement stems from its more accurate representation of the near-wall velocity gradient, which has an appreciable bearing on the wall shear stress.

A comparable pattern emerges in Fig. 2b, where the percent error in boundary-layer thickness is reported. While the classical Pohlhausen profile provides reasonable thickness estimates for shear-thinning fluids, the MX4 formulation maintains improved agreement as n approaches unity and beyond. Indeed, the MX4 profile surpasses Pohlhausen's approximation for $n \gtrsim 0.84$, reflecting its enhanced representation of the wall-gradient parameter and its connection to streamwise growth of the disturbance thickness.

The role of the wall-gradient parameter becomes more transparent upon examining Fig. 3a. The similarity solution enables us to determine the value of $f''(0)$, which controls the wall shear stress and, consequently, the local skin-friction coefficient [11, 38]. As shown in this graph, $f''(0)$ varies systematically with n, thus showcasing the effect of nonlinear viscosity on the near-wall velocity field. Because the wall shear stress enters directly into the momentum-integral equation, variations in $f''(0)$ propagate into the predicted rate of boundary-layer growth. They appear in the evaluation

Table 1. Boundary-layer parameters from similarity, Pohlhausen, and MX4 solutions

	Exact Similarity [8, 9]			KP4 [21]			MX4 [26]		
n	α	β	H	α	β	H	α	β	H
0.6	0.2689	0.1136	2.368	0.300	0.1175	2.554	0.350	0.1337	2.618
0.8	0.3158	0.1262	2.501	0.300	0.1175	2.554	0.350	0.1337	2.618
1.0	0.3442	0.1328	2.591	0.300	0.1175	2.554	0.350	0.1337	2.618
1.2	0.3759	0.1416	2.654	0.300	0.1175	2.554	0.350	0.1337	2.618
1.4	0.3948	0.1462	2.701	0.300	0.1175	2.554	0.350	0.1337	2.618

Table 2. Boundary-layer growth and skin-friction scaling constants relative to the similarity solution. Percent errors are reported for the integral methods

	Exact Similarity [8, 9]			KP4 [21]				MX4 [26]			
n	δ/x	C_f	δ^*/x	δ/x	C_f	$\%\Delta\delta$	$\%\Delta C_f$	δ/x	C_f	$\%\Delta\delta$	$\%\Delta C_f$
0.6	7.1509	1.0168	1.9232	6.6341	0.9741	7.23	4.20	5.7143	0.9549	20.09	6.08
0.8	5.7812	0.8109	1.8255	6.1992	0.8091	7.23	0.23	5.3202	0.7903	7.98	2.55
1.0	5.0000	0.6641	1.7208	5.8356	0.6855	16.71	3.21	4.9934	0.6676	0.13	0.52
1.2	4.3195	0.5561	1.6237	5.5287	0.5904	27.99	6.16	4.7194	0.5736	9.26	3.14
1.4	3.8937	0.4743	1.5373	5.2671	0.5156	35.27	8.70	4.4871	0.4999	15.24	5.40

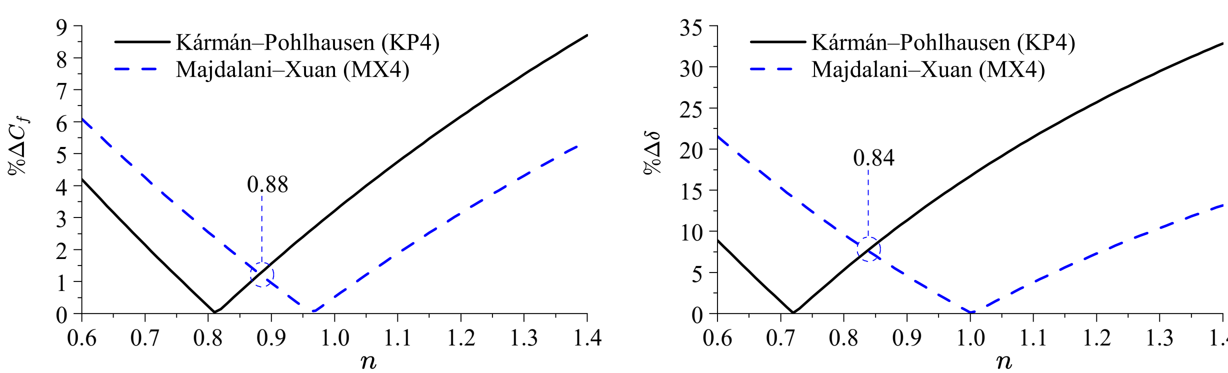

a) Skin-friction error

b) Boundary-layer thickness error

Fig. 2. Percent error in a) skin friction and b) disturbance thickness relative to the Schowalter–Acrivos similarity solution using the KP4 and MX4 velocity profiles across a wide range of power-law indices.

of C_f in Eq. (9). Using $n = 1$, for instance, one extracts $f''(0) \approx 0.332$ from Fig. 3a, which enables us to readily restore the $C_f\sqrt{Re_x} = 0.664$ classic value for a Newtonian fluid by way of Fig. 3a.

As the flow-behavior index increases, the constitutive relation amplifies the sensitivity of wall shear stress to the near-wall velocity gradient. Consequently, even modest discrepancies in the assumed wall gradient produce increasingly pronounced deviations in both C_f and δ for shear-thickening fluids. Conversely, shear-thinning regimes exhibit reduced sensitivity to gradient misrepresentation, rendering the classical Pohlhausen profile comparatively more robust in that range.

The transverse velocity shown in Fig. 3b follows the same dependence on the flow behavior index observed in the thickness and skin-friction results. As n increases, the normalized form of the transverse velocity decreases. In this shear-thickening range, the reduced cross-stream entrainment is consistent with the diminished boundary-layer growth and C_f reported in Table 2. In contrast, shear-thinning flows are found to exhibit a more prominent transverse motion. The MX4 profile remains closer to the similarity solution near and above $n = 1$, whereas the classical Pohlhausen formulation performs better in deeper shear-thinning cases, which is consistent with prior trends. These results reflect the strong coupling between near-wall gradients, streamwise growth, and cross-stream transport.

Overall, the results demonstrate that the predictive fidelity of integral boundary-layer approximations depends jointly on the rheological regime and the near-wall velocity representation. The Pohlhausen quartic profile provides reliable estimates for shear-thinning flows, whereas the optimized MX4 formulation offers improved accuracy in Newtonian and shear-thickening regimes. These findings are consistent with the conclusions of Majdalani and Xuan [26], particularly, that careful optimization of polynomial velocity distributions can substantially enhance the model's agreement with similarity-based solutions without sacrificing analytical tractability.

IV. Conclusions

In this work, integral boundary-layer approximations for the laminar flow of an incompressible power-law fluid over a flat plate are developed using the Kármán–Pohlhausen momentum-integral framework in conjunction with two quartic velocity representations: the classical Pohlhausen profile (KP4) and the optimized Majdalani–Xuan (MX4) polynomial. Closed-form analytical expressions are derived for the disturbance thickness, displacement, and momentum thicknesses, as well as the local skin-friction coefficient as functions of the streamwise coordinate, consistency coefficient, and flow-behavior index. These predictions are systematically evaluated against the generalized Schowalter–Acrivos similarity solution, which serves as the reference model.

The comparison reveals that the predictive fidelity of the integral formulation depends primarily on the representation of the near-wall velocity gradient and, secondarily, on the rheological regime characterized by the flow-behavior index, n. Near the Newtonian limit, both quartic profiles recover the classical boundary-layer scaling with minimal deviation. As the flow departs from $n = 1$, however, the performance of each profile becomes increasingly regime dependent.

For shear-thinning fluids with $n < 1$, the classical Pohlhausen polynomial remains competitive and, in several cases,

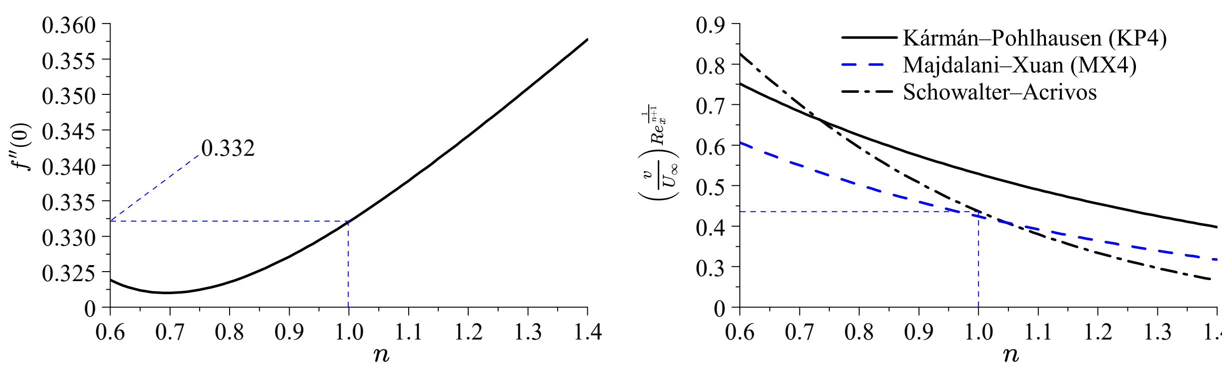

a) Similarity wall gradient parameter

b) Normalized wall-normal velocity

Fig. 3. Sensitivity of a) the similarity wall-gradient parameter, $f''(0)$, as well as b) the normalized wall-normal velocity, $\hat{v} = vRe_x^{1/(n+1)}/U_\infty$, evaluated at $\eta = 1/2$, across a wide range of power-law indices.

exhibits smaller deviations in both disturbance thickness and skin friction (i.e., for $n < 0.84$ and $n < 0.88$, respectively). Conversely, as the flow approaches Newtonian and shear-thickening behavior ($n \geq 1$), the MX4 formulation provides consistently improved agreement with the similarity solution. This enhanced performance is directly attributable to its optimized wall-gradient parameter, which more accurately captures the shear stress gradient affecting the momentum-integral relation. In practice, it outperforms Pohlhausen's KP4 formulation in estimating the boundary-layer thickness and skin-friction coefficient for $n \geq 0.84$ and $n \geq 0.88$, respectively.

The role of the similarity wall-gradient parameter, $f''(0)$, becomes especially evident in dilatant regimes. Because the wall shear stress scales with the velocity gradient raised to the power n, even modest discrepancies in the assumed near-wall slope are amplified as n is increased. Consequently, shear-thickening flows are seen to exhibit heightened sensitivity to polynomial structure, whereas shear-thinning fluids seem to entail comparatively reduced dependence on wall gradient precision.

These findings suggest that the principal limitation of classical Kármán–Pohlhausen formulations in non-Newtonian boundary layers arises not from the integral framework itself, but from the assumed velocity distribution embedded within it. When the near-wall behavior is represented with sufficient fidelity, the momentum-integral method is likely to remain both robust and analytically tractable across a broad range of rheological conditions. For this reason, the development of rheologically-sensitive nearfield profiles that incorporate the effect of n are presently needed.

From a practical standpoint, the foregoing results provide clear guidance for engineering applications involving non-Newtonian drag estimation and boundary-layer analysis. On the one hand, the classical Pohlhausen profile offers an analytically simple and sufficiently accurate approximation for shear-thinning fluids. On the other hand, for Newtonian and shear-thickening regimes, where wall-shear sensitivity is amplified, the MX4 formulation offers superior predictive capability without sacrificing closed-form convenience. The continued use of integral methods is therefore well justified, provided that the assumed velocity representation is selected in accordance with the rheological model in question.

References

[1] White, F. M. and Majdalani, J., *Viscous Fluid Flow*, McGraw-Hill, New York, 4th ed., 2021.

[2] Prandtl, L., "Über Flüssigkeitsbewegung bei sehr kleiner Reibung," *Proceedings of the Third International Mathematical Congress Heidelberg*, 1904, NACA Technical Memo. 452.

[3] Blasius, H., "Grenzschichten in Flüssigkeiten mit kleiner Reibung," *Journal of Applied Mathematics and Mechanics (ZAMM)*, Vol. 56, 1908, pp. 1–37.

[4] Tani, I., "History of Boundary Layer Theory," *Annual Review of Fluid Mechanics*, Vol. 9, January 1977, pp. 87–111. doi:10.1146/annurev.fl.09.010177.000511.

[5] Kays, W. M., Crawford, M. E., and Weigand, B., *Convective Heat and Mass Transfer*, McGraw-Hill, New York, NY, 4th ed., 2005.

[6] Cebeci, T. and Bradshaw, P., *Momentum Transfer in Boundary Layers*, McGraw-Hill, 1977.

[7] Schlichting, H., *Boundary Layer Theory*, McGraw–Hill, New York, 7th ed., 1979.

[8] Schowalter, W. R., "The Application of Boundary Layer Theory to Power Law Pseudoplastic Fluids: Similar Solutions," *American Institute of Chemical Engineers Journal*, Vol. 6, 1960, pp. 24–28.

[9] Acrivos, A., Shah, M. J., and Petersen, E. E., "Momentum and Heat Transfer in Laminar Boundary Layer Flow of Non-Newtonian Fluids Past External Surfaces," *American Institute of Chemical Engineers Journal*, Vol. 6, 1960, pp. 312–317.

[10] Hansen, A. G., *Fluid Mechanics*, Wiley, New York, 1967.

[11] Khan, W. A., Culham, J. R., and Yovanovich, M. M., "Fluid Flow and Heat Transfer in Power-Law Fluids Across Circular Cylinders: Analytical Study," *Journal of Heat Transfer*, Vol. 128, No. 9, September 2006, pp. 870–878. doi:10.1115/1.2241747.

[12] Bharti, R. P., Sivakumar, P., and Chhabra, R. P., "Forced Convection Heat Transfer from an Elliptical Cylinder to Power-Law Fluids," *International Journal of Heat and Mass Transfer*, Vol. 51, No. 7–8, April 2008, pp. 1838–1853. doi:10.1016/j.ijheatmasstransfer.2007.06.032.

[13] Rao, P. K., Sahu, A. K., and Chhabra, R. P., "Flow of Newtonian and Power-Law Fluids Past an Elliptical Cylinder: A Numerical Study," *Industrial and Engineering Chemistry Research*, Vol. 49, No. 14, June 2010, pp. 6649–6661. doi:10.1021/ie100251w.

[14] Chhabra, R. P., *Fluid Flow and Heat Transfer from Circular and Noncircular Cylinders Submerged in Non-Newtonian Liquids*. Elsevier, 2011, pp. 289–417. doi:10.1016/b978-0-12-381529-3.00004-9.

[15] Chhabra, R. P., "Laminar Boundary Layer Heat Transfer to Power Law Fluids: An Approximate Analytical Solution," *Journal of Chemical Engineering of Japan*, Vol. 32, No. 6, 1999, pp. 812–816.

[16] Chhabra, R. P. and Richardson, J. F., *Non-Newtonian Flow and Applied Rheology*, Butterworth-Heineman, 2nd ed., 2008.

[17] Myers, T. G., "An Approximate Solution Method for Boundary Layer Flow of a Power Law Fluidover a Flat Plate," *International Journal of Heat and Mass Transfer*, Vol. 53, No. 11, Nov. 2010, pp. 2337–2346. doi:10.1016/j.ijheatmasstransfer.2010.02.006.

[18] Andersson, H. I. and Toften, T. H., "Numerical Solution of the Laminar Boundary-Layer Equations for Power-Law Fluids," *Journal of Non-Newtonian Fluid Mechanics*, Vol. 32, No. 2, 1989, pp. 175–195.

[19] Huang, M. J. and Chen, C. K., "Numerical Analysis for Forced Convection over a Flat Plate in Power Law Fluids," *International Communications in Heat and Mass Transfer*, Vol. 11, No. 4, 1984, pp. 361–368.

[20] von Kármán, T., "Über laminare und turbulente Reibung," *Journal of Applied Mathematics and Mechanics (ZAMM)*, Vol. 1, No. 4, 1921, pp. 233–252. doi:10.1002/zamm.19210010401.

[21] Pohlhausen, K., "Zur näherungsweisen Integration der Differentialgleichung der laminaren Grenzschicht," *Journal of Applied Mathematics and Mechanics (ZAMM)*, Vol. 1, No. 4, 1921, pp. 252–290. doi:10.1002/zamm.19210010402.

[22] Schlichting, H. and Gersten, K., *Boundary-Layer Theory*, Springer-Verlag, Berlin, 9th ed., 2017.

[23] White, F. M., *Viscous Fluid Flow*, McGraw-Hill, New York, 3rd ed., 2006.

[24] Cebeci, T. and Cousteix, J., *Modeling and Computation of Boundary-Layer Flows*, Horizons, Long Beach, Calif, 1998.

[25] Khan, W. A., Culham, J. R., and Yovanovich, M. M., "Fluid Flow Around and Heat Transfer From an Infinite Circular Cylinder," *Journal of Heat Transfer*, Vol. 127, 2005, pp. 785–790. doi:10.1115/1.1924629.

[26] Majdalani, J. and Xuan, L.-J., "On the Kármán Momentum Integral Approach and the Pohlhausen Paradox," *Physics of Fluids*, Vol. 32, No. 12, December 2020, pp. 123605. doi:10.1063/5.0036786.

[27] Nakayama, A., Shenoy, A. V., and Koyama, H., "An analysis for forced convection heat transfer from external surfaces to non-Newtonian fluids," *Wärme- und Stoffübertragung*, Vol. 20, 1986, pp. 219–227. doi:10.1007/BF01303454.

[28] Shenoy, A. V. and Nakayama, A., "Forced convection heat transfer from axisymmetric bodies to non-Newtonian fluids," *The Canadian Journal of Chemical Engineering*, Vol. 64, No. 4, 1986, pp. 680–686. doi:10.1002/cjce.5450640420.

[29] Nakayama, Y., *Visualized flow: Fluid Motion in Basic and Engineering Situations Revealed by Flow Visualization*, Pergamon, Oxford New York, 1988.

[30] Mehta, K. N. and Sood, S., "Free Convection About Axisymmetric Bodies Immersed in Inhomogeneous Porous Medium," *International Journal of Engineering Science*, Vol. 32, 1994, pp. 945–953. doi:10.1016/0020-7225(94)90048-5.

[31] Nakayama, A. and Pop, I., "Free Convection Over a Nonisothermal Body in a Porous Medium with Viscous Dissipation," *International Communications in Heat and Mass Transfer*, Vol. 16, 1989, pp. 173–180. doi:10.1016/0735-1933(89)90018-3.

[32] Bujurke, N. M. and Jagadeeswar, M., "Momentum Integral Method in the Analysis of Taper-Flat Slider Bearing with Second-Order Fluid," *Journal of Applied Mathematics and Mechanics (ZAMM)*, Vol. 72, No. 3, March 1992, pp. 225–228. doi:10.1002/zamm.19920720309.

[33] Rao, A. and Arakeri, J. H., "Integral Analysis Applied to Radial Film Flows," *International Journal of Heat and Mass Transfer*, Vol. 41, 1998, pp. 2757–2767. doi:10.1016/S0017-9310(98)00375-5.

[34] Mustapha, A. and Mohand, K., "On Cauchy Conditions for Asymmetric Mixed Convection Boundary Layer Flows," *International Journal of Thermal Sciences*, Vol. 42, 2003, pp. 621–630. doi:10.1016/S1290-0729(03)00027-9.

[35] Denier, J. P. and Dabrowski, P. P., "On the Boundary-Layer Equations for Power-Law Fluids," *Proceedings of the Royal Society of London. Series A: Mathematical, Physical and Engineering Sciences*, Vol. 460, 2004, pp. 3143–3158.

[36] Hsu, C.-C., "A Simple Solution for Boundary Layer Flow of Power Law Fluids Past a Semi-Infinite Flat Plate," *American Institute of Chemical Engineers Journal*, Vol. 15, No. 3, 1969, pp. 367–370.

[37] von Kármán, T., "Über den Mechanismus des Widerstandes, den ein bewegter Körper in einer Flüssigkeit erzeugt," *Nachrichten von der Gesellschaft der Wissenschaften zu Göttingen, Mathematisch-physikalische Klasse II*, 1911, pp. 509–517, 547–556.

[38] Schlichting, H. and Gersten, K., *Boundary Layer Theory*, Springer, New York, 8th ed., 2000.

[39] Mitchell, J. W., McDonald, A. T., and Fox, R. W., *Fox and McDonald's Introduction to Fluid Mechanics*, John Wiley & Sons, Hoboken, NJ, 10th ed., 2020.

[40] Swafford, T. W., "Analytical Approximation of Two-Dimensional Separated Turbulent Boundary-Layer Velocity Profiles," *AIAA Journal*, Vol. 21, No. 6, June 1983, pp. 923–926. doi:10.2514/3.8177.

[41] Majdalani, J. and Shelton, C. M., "On Prandtl's Turbulent Flow Expressions for Arbitrary Power-Law and Shear-Stress Exponents," *Physics of Fluids*, Vol. 37, No. 8, August 2025, pp. 085117. doi:10.1063/5.0270261.

[42] Al Ahmar, R. and Majdalani, J., "On the Kármán Momentum-Integral Approach and the Pohlhausen Paradox: Extension to a Cylinder in Crossflow with a Potential Farfield Motion," *Physics of Fluids*, Vol. 34, No. 6, June 2022, pp. 063107. doi:10.1063/5.0096780.

[43] Al Ahmar, R., Majdalani, J., and Sharma, G., "Improved Viscous and Thermal Boundary-Layer Formulations for a Cylinder in Crossflow Using Kármán's Momentum-Integral Approach," *International Journal of Heat and Mass Transfer*, Vol. 240, No. 5, May 2025, pp. 126474. doi:10.1016/j.ijheatmasstransfer.2024.126474.